1993

Examination of Separation Efficiencies of Mercury Vapour for Different Gas-Liquid Separators in Flow Injection Cold Vapour Atomic Absorption Spectrometry with Amalgam Preconcentration

C. P. Hanna
University of Massachusetts Amherst

P. E. Haigh
University of Massachusetts Amherst

Julian Tyson
University of Massachusetts Amherst

S. McIntosh

Examination of Separation Efficiencies of Mercury Vapour for Different Gas–Liquid Separators in Flow Injection Cold Vapour Atomic Absorption Spectrometry with Amalgam Preconcentration

C. P. Hanna*, P. E. Haigh and J. F. Tyson†
Chemistry Department, University of Massachusetts Amherst, MA 01003, USA

S. McIntosh
Inorganic Analysis Division, Perkin-Elmer Corporation, 761 Main Avenue, Norwalk, CT 06859, USA

A comparison has been made of the separation efficiency of three designs of gas–liquid separator when used in a flow injection (FI) manifold for the determination of Hg by cold vapour atomic absorption spectrometry. The manifold used with each device was separately optimized for maximum sensitivity. This involved studies of the effects of reagent flow rates, argon purge gas flow rate, injection time and post-injection purge time. A significant difference, with respect to both peak height and integrated signal sensitivity (by a factor of approximately 3) between the performance of a miniature design and that of two larger volume designs was obtained. No significant differences in precisions were observed. For the miniature design, the use of either tetrahydroborate or tin(II) reductant was investigated. No difference in peak height sensitivity was found, but the integrated signal sensitivity for the tetrahydroborate was 36% lower. The efficiency of separation was measured by comparison of the signal obtained from a known mass of Hg vapour, introduced *via* an amalgam preconcentration unit, and the signal obtained from a known mass of Hg in solution, introduced *via* the FI manifold and amalgam preconcentration unit. The efficiencies were found to be 101 ± 4% and 103 ± 6% for peak height and integrated signal, respectively.

Keywords: *Flow injection cold vapour atomic absorption spectrometry; gas–liquid separator; efficiency study*

The use of continuous flow (CF) and flow injection (FI) analysis for the determination of Hg by cold vapour atomic absorption spectrometry (CVAAS) has been the subject of study for a number of years.[1–17] The various methods described can differ greatly, with little conformity between them. While some methods determine the total Hg present in a sample,[1–3,5,8,11,12,16,17] others appear to render only information about the amounts of inorganic Hg in the sample.[4,7,13,14] Some investigators use tin(II) as the reductant,[1–5,7,8,11–16] while others use sodium or potassium tetrahydroborate.[6,9,10,17] Sodium or potassium tetrahydroborate is presumably used because of the rapid reaction kinetics and the ability to reduce organic Hg compounds to elemental Hg. However, recent findings have shown that sodium tetrahydroborate does not reduce all organic Hg compounds to the same extent.[18]

One component of CF- and FI-CVAAS that demonstrates virtually no conformity is that of the gas–liquid separator (GLS) employed in the system. Some practitioners of FI-CVAAS have utilized a microporous poly(tetrafluoroethylene) (PTFE) membrane material as a diffusion medium for the separation of the Hg vapour from solution.[6,9,10] While these membrane separators have yielded excellent results, their mechanical stability and resilience over time, in addition to their uniformity in composition, are areas that require attention before wide-scale acceptance of them is achieved.

Most investigators of CF- and FI-CVAAS have used some sort of open chamber (typically made of glass) in which the reaction products are separated by employing an inert purge gas. The designs of the separators are as variable as are the methods described. For example, investigators have used devices which range from miniaturized Vijan-type U-tubes[10] and open chambers, into which reaction products and purge gas are added separately,[14] to chambers in which the flow of reaction products is directed to the surface of a sintered glass frit for purging.[4] The systems that employ these GLSs all exhibit varying degrees of sensitivity, with no apparent agreement being reached as to the optimum GLS design. Only two investigations have been made into the comparison of GLS designs for their effect on separation capability, in which PTFE membrane separation in FI hydride generation for inductively coupled plasma atomic emission detection was examined.[19,20] It has been noted,[9,10] however, and is generally agreed upon, that the reduction of the internal volume of the GLS is of greater importance in FI systems than in CF systems. Since FI involves the injection of a discrete sample, a large volume GLS will lead to greater dispersion of the analyte zone prior to detection, whereas a CF analyte zone will ultimately reach a maximized steady state regardless of GLS volume.

A recent development in CF- and FI-CVAAS technology has been that of an amalgam accessory for the determination of Hg. The principle behind the amalgam accessory is that the liberated Hg vapour is trapped on the surface of gold–platinum gauze or gold-covered sand packed into a quartz tube. This packed area of the quartz tube is then rapidly heated and the released Hg vapour is conducted to an atomic spectrometer for detection. Less than 50 pg of Hg can be detected in an optimized system when AAS is applied.[21] Since the kinetics of Hg desorption are consistent from one heating cycle to the next, the signal then becomes dependent only upon the mass of Hg introduced onto the trapping surface and is independent of the kinetic processes occurring before the trapping surface. Thus, when the amalgam accessory is used in conjunction with CF- and FI-CVAAS procedures, the sensitivity is dependent only upon the efficiency of separation achieved with the GLS being used. Therefore, large gas-phase dilution factors for the Hg vapour due to large volume GLSs or high purge gas flow rates can effectively be reversed. Maximum sensitivity will then be approached if a particular GLS approaches 100% separation efficiency.

The aim of this work is to illustrate the variation of separation efficiencies for Hg vapour when three GLSs of different design are used. It is hypothesized that if a given GLS achieves 100% separation efficiency using an optim-

*Present address: Inorganic Analysis Division, Perkin-Elmer Corporation, 761 Main Avenue, Norwalk, CT 06859, USA.
†To whom correspondence should be addressed.

ized manifold with amalgam preconcentration, the sensitivity obtained is maximized. By using amalgam preconcentration, the kinetic process occurring in the manifold, which would otherwise lead to a decrease in sensitivity, are now decoupled from the atomic spectrometer. Manifold conditions for each GLS were optimized prior to comparisons. The most efficient conditions with the most efficient GLS were then used to determine the separation efficiency relative to a source of Hg vapour of known vapour phase concentration.

Experimental

Instrumentation

An FIAS 200 flow injection atomic spectrometry system supplied by Perkin-Elmer was used throughout the study. This system consisted of pumps, pump tubing, connecting tubing (1.0 mm i.d. Teflon), injection valve, manifold connections and argon regulation (0–250 ml min^{-1}). This system was used in conjunction with a Perkin-Elmer 3100 atomic absorption spectrometer. A hollow cathode lamp (Perkin-Elmer) drawing 6 mA of current was used as the atomic line source and the spectrometer was tuned to the 253.7 nm line, with a spectral bandpass of 0.7 nm and a low slit setting.

A Perkin-Elmer amalgam system was used for the trapping of the liberated Hg vapour. This system supplies both an argon purge gas for the manifold and an argon carrier gas for the desorbed Hg. The trapping medium is a 1.2 cm long plug of rolled gold–platinum gauze inserted into a length of quartz tube (0.3 cm i.d.). The gold gauze was rapidly heated by activating two 10 W tungsten filament lamps facing one another around the gauze. The system was cooled by compressed air, which was delivered under controlled timing.

Analysis parameters, such as pump speed, argon flow rate, purge time and injection time, were controlled through Perkin-Elmer FIAS software, run on a Digital DECStation PC. Data collection and data treatment were also controlled through the Perkin-Elmer FIAS software.

Reagents

All solutions were prepared with distilled, de-ionized water produced by an E-Pure System (Barnstead). Hydrochloric acid carrier stream solutions were prepared by diluting an appropriate amount of concentrated hydrochloric acid (ACS grade, 36.5% m/m, Fisher Scientific) to concentrations expressed as % v/v with distilled, de-ionized water. Tin(II) chloride reductant solution (10% m/v) was prepared by dissolving 50.0 g of tin(II) chloride dihydrate (Fisher Scientific) in 50 ml of concentrated hydrochloric acid and diluting to 500 ml with distilled, de-ionized water. Sodium tetrahydroborate reductant solution (1% m/v) was prepared by dissolving 5.0 g of sodium tetrahydroborate powder (Fisher Scientific) in 500 ml of 0.05% m/v sodium hydroxide (from pellets, Fisher Scientific) solution. These reductant solutions were purged with argon for 30 min prior to use. Standard solutions were prepared by diluting a 1000 mg l^{-1} standard solution of Hg^{II} (Fisher Scientific) to a concentration of 20 ng ml^{-1}. This standard was preserved with 10% hydrochloric acid or with 0.5% nitric acid–0.005% potassium dichromate.

Gas–Liquid Separators

Three differently designed gas–liquid separators were chosen for examination. The first GLS was supplied by Perkin-Elmer in the FIAS 200 system for Hg and hydride generation analysis procedures (referred to as PE). This GLS is shown in Fig. 1(*a*). The PE consists of a cylindrical chamber of 0.8 cm i.d. and 3.0 cm height, one third filled with 0.3 cm diameter glass beads. The reaction products and purging argon enter through a side arm, with the argon and Hg passing through an opening in the top of the GLS and the spent liquid being pumped to waste through a second side arm.

The second and third GLSs were obtained from PS Analytical (Sevenoaks, Kent, UK). One was a GLS designed specifically for sodium tetrahydroborate reductions in hydride generation and Hg cold vapour generation[22] (referred to as PSA1), and the other was designed for tin(II) chloride reductions exclusively in Hg cold vapour generation (referred to as PSA2). The PSA1 is shown in Fig. 1(*b*) and PSA2 is shown in Fig. 1(*c*). The PSA1 consists of a cylindrical chamber with a U-tube drain attached at the bottom, so that a constant level of solution is sustained in the chamber. Two glass tubes feed into the chamber, one for reaction products and one for the argon purge gas. The PSA2 is similar to PSA1 in its cylindrical chamber and U-tube design. However, the reaction products in PSA2 enter through a side arm of the chamber and a glass tube for the argon purge opens below the surface of the liquid.

Procedure

Each GLS was optimized separately from maximum separation efficiency, which was determined as the maximum signal arising from applying the amalgam trapping accessory. Each GLS was put in line with a constant manifold, shown in Fig. 2, and the variables of reagent flow rate, argon

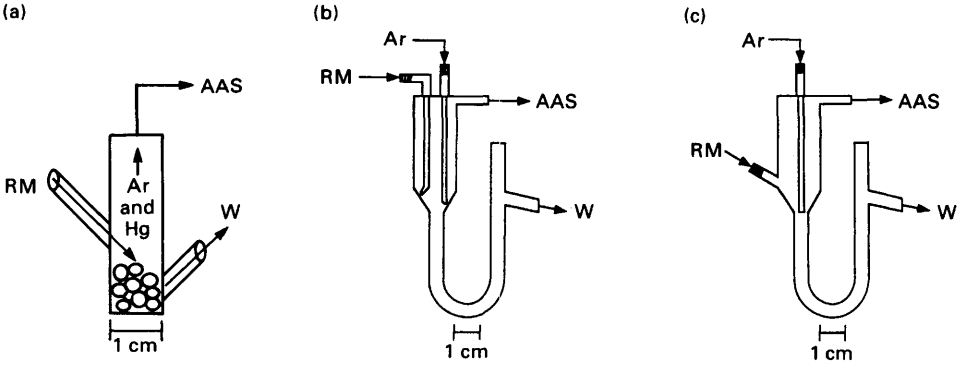

Fig. 1 Design of the three gas–liquid separators (GLSs) examined: (*a*) Perkin-Elmer GLS designed for sodium tetrahydroborate and tin(II) chloride reductions; (*b*) PS Analytical GLS designed for sodium tetrahydroborate reductions; and (*c*) PS Analytical GLS designed for tin(II) chloride reductions. W = waste and RM = reaction mixture

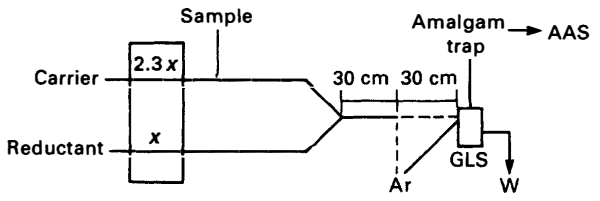

Fig. 2 Manifold used for examination of GLS efficiencies. The broken lines indicate slight modifications in the manifold to accommodate the PE GLS, since argon is added directly to the manifold for this GLS and not for the others

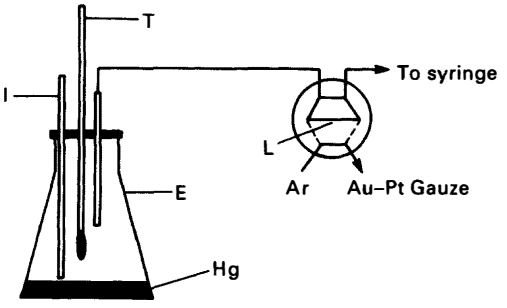

Fig. 3 Design of apparatus used for introducing a known mass of Hg vapour to the amalgam system. E, 125 ml Erlenmeyer flask; I, 2 mm i.d. PTFE inlet tube for pressure equilibration; T, thermometer; and L, 500 μl sample loop. This loop is filled with the mercury-saturated headspace of the Erlenmeyer by retracting the plunger of a 5 ml syringe. This known mass of mercury vapour is then injected into an argon carrier and then onto the Au–Pt gauze

purge flow rate, injection time (the amount of time the injection valve remained in the 'inject' position with the argon purge gas activated, T_i) and post-injection purge time (the amount of time after the injection valve was returned to the 'load' position and the argon purge continued, T_p), were optimized by applying a single cycle alternating variable search procedure. The effect of reagent flow rate and argon purge flow rate were also examined for their effect on the signal without the amalgam trapping accessory, using the PE GLS. This part of the optimization utilized 10% v/v hydrochloric acid as the standard solution preservative and as the carrier stream, and 10% m/v tin(II) as the reductant. Once the optimum conditions were determined for each GLS they were compared directly with one another at their respective optimized conditions.

The most efficient GLS was then used to examine the effects of carrier acidity on the signal and the blank values, the contribution by the standard solution preservative to the signal and the blank values, and how the signal obtained with this GLS compared with that obtained from a known mass of Hg vapour introduced into the amalgam system. This known mass was introduced by using the apparatus shown in Fig. 3, which is similar to systems previously described.[23–25] The effect of the type of reductant used was then examined by employing 1% m/v sodium tetrahydroborate solution with the optimized conditions determined above, using the most efficient of the three GLSs and comparing the efficiency obtained with that achieved using the tin(II) reductant.

Results and Discussion

Effect of Reagent Flow Rate

For all of the GLSs examined, the speed of the pump used for propelling the reagents was varied from 40 to 120 rev min^{-1} (5–15 ml min^{-1} total flow rate), with the argon flow rate constant at 250 ml min^{-1}, injection time constant at 25 s and the post-injection purge time constant at 30 s.

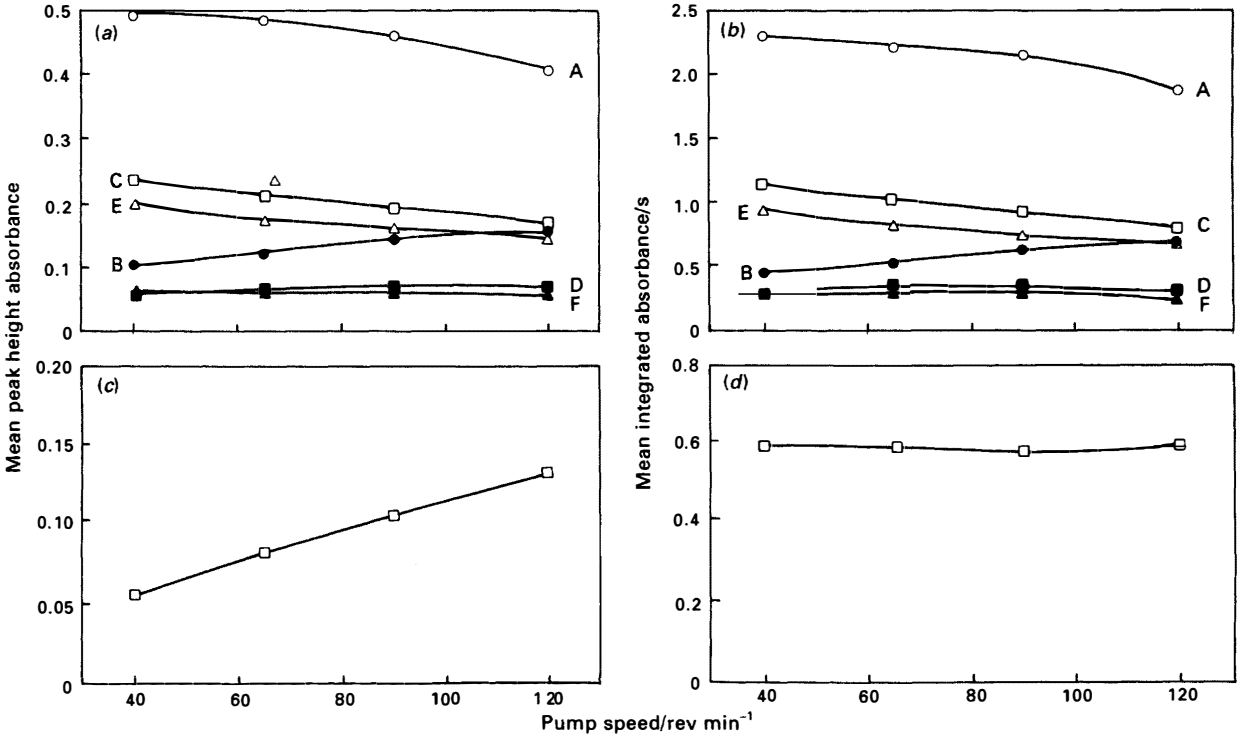

Fig. 4 Effect of pump speed on the efficiency of separation for a 500 μl sample of 20 ng ml^{-1} of Hg^{II}. Argon flow is constant at 250 ml min^{-1}, T_i is constant at 25 s and T_p is constant at 30 s: (*a*) peak height measurements and (*b*) integrated signal. A, PE signal; B, PE blank; C, PSA1 signal; D, PSA1 blank; E, PSA2 signal; and F, PSA2 blank. The effect of pump speed when the amalgam accessory is not used with the PE GLS is also shown for (*c*) peak height measurements and (*d*) integrated signal

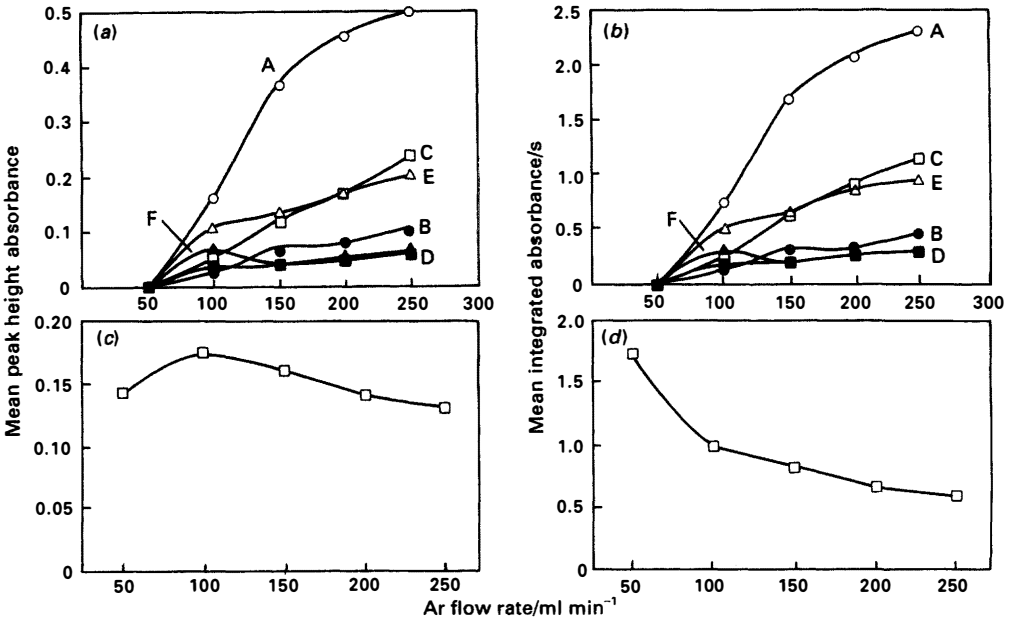

Fig. 5 Effect of argon purge flow rate on the efficiency of separation for a 500 μl sample of 20 ng ml^{-1} of Hg^{II}. Pump speed is constant at 40 rev min^{-1} (5 ml min^{-1}), T_i is constant at 25 s, and T_p is constant at 30 s: (*a*) peak height measurements and (*b*) integrated measurements. A, PE signal; B, PE blank; C, PSA1 signal; D, PSA1 blank; E, PSA2 signal; and F, PSA2 blank. The effect of argon purge flow rate when the amalgam accessory is not used with the PE GLS is also shown for (*c*) peak height measurements and (*d*) integrated signal

For all three GLSs examined, both peak height and integrated signal sensitivity increased with decreased pump speed, while the associated blank values decreased for decreased pump speed. This trend is shown in Fig. 4(*a*) and (*b*). These observations can be explained in two ways: (*i*) for a fixed time the decreased pump speed allows for an increased residence time of the sample in the manifold prior to separation, thus, the reduction of Hg^{II} to Hg has more time to go to completion and more Hg vapour is liberated as an end result; and (*ii*) for a fixed time, the decreased pump speed results in less background Hg from the carrier and reductant streams entering the GLS, thus, decreasing blank values.

When the amalgam accessory is not used and the reagent flow rate is varied in the same range, the signal is effected in an entirely different way, as shown in Fig. 4(*c*) and (*d*). While the integrated signal remains about the same throughout the range, peak height shows a substantial decrease for lower reagent flow rates. The increased dispersion of the sample zone at lower reagent flow rates thus leads to a shorter signal that is more spread out over time. This effect is therefore effectively reduced by using amalgamation prior to detection.

Effect of Argon Purge Flow Rate

For all of the GLS examined, the effect of argon purge flow rate was examined from 50 to 250 ml min^{-1}. The pump speed was constant at 40 rev min^{-1}, injection time was constant at 25 s and post-injection purge time was constant at 30 s. The maximum argon purge flow rate examined was 250 ml min^{-1} for two reasons: (*i*) due to back-pressure limitations, the requirement of adding argon to the manifold and not the GLS for the PE GLS resulted in a maximum argon flow rate of 250 ml min^{-1}; and (*ii*) and argon flow rate greater than 250 ml min^{-1} in the two PSA GLSs resulted in liquid being violently forced out of the draining end of the U-tube, resulting in virtually no reaction products collecting in the GLS chambers.

For all of the GLSs, peak height and integrated signal sensitivity increased with increased argon flow rate, as did the blank values obtained. This trend is shown in Fig. 5(*a*) and (*b*). While this argon increase led to a decrease in sensitivity for a system not using amalgam trapping due to increased analyte zone dispersion in the gas phase and decreased residence time in the atom cell, Fig. 5(*c*) and (*d*), this is reversed by trapping and refocusing the analyte zone prior to desorption and detection.

Effect of Injection Time (T_i)

The effect of the length of time the injection valve was kept in the 'inject' position, T_i, was investigated to ensure that the entire sample zone was emerging from the sample loop. The manufacturer's recommended T_i of 25 s (T_p = 30 s, total purge time 55 s) and a T_i of 50 s (T_p = 5 s, total purge time 55 s) were investigated. It was found that there was virtually no difference in the signal, blank or blank-subtracted signal for increasing T_i. It was decided to leave the value of T_i at 25 s.

Effect of Post-injection Purge Time (T_p)

The effect of post-injection purge time, T_p, was examined from 5 to 30 s for the PE and PSA1 GLS and from 2 to 30 s for the PSA2 GLS. While there was a general decrease in both signal and blank values obtained for decreased T_p, there was a maximum in the blank-subtracted signals for each GLS. Thus, an optimized T_p corresponds to a time where the maximum amount of the sample zone is entering the GLS with a minimum amount of the Hg background-containing carrier stream. The PE GLS produced a blank-subtracted signal maximum for a T_p of 5–10 s and the PSA2 GLS produced a maximum at T_p = 10 s. However, the PSA1 GLS had a higher T_p for maximum blank-subtracted sensitivity at 30 s, presumably due to the longer time period required for the complete emergence of the sample zone into the GLS because of the glass tube which extends into the PSA1 GLS chamber. This trend is shown in Fig. 6.

Comparison of PE, PSA1 and PSA2 GLSs

The three GLSs examined were directly compared with one another at their respective optimized parameters of pump

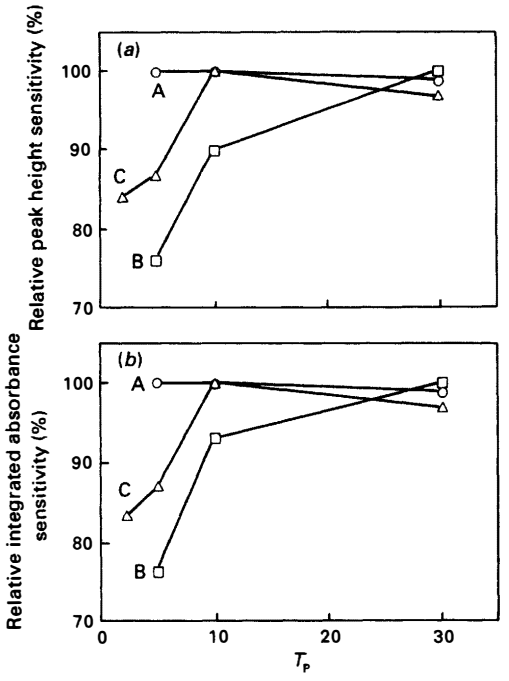

Fig. 6 Effect of T_p on the efficiency of separation for a 500 μl sample of 20 ng ml^{-1} of Hg^{II}. Pump speed is constant at 40 rev min^{-1} (5 ml min^{-1}), T_i is constant at 25 s and argon flow is constant at 250 ml min^{-1}. The maximum blank-corrected signal for each GLS is expressed as 100% relative sensitivity: (*a*) peak height measurements and (*b*) integrated signal for A, PE; B, PSA1; and C, PSA2

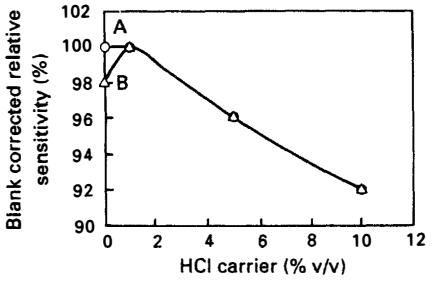

Fig. 7 Effect of carrier acidity on the efficiency of separation for a 500 μl sample of 20 ng ml^{-1} of Hg^{II}, using the PE GLS. Pump speed is constant at 40 rev min^{-1} (5 ml min^{-1}), T_i is constant at 25 s, T_p is constant at 10 s, and argon flow is constant at 250 ml min^{-1}. The maximum blank-corrected signals for A, peak height; and B, integrated absorbance are expressed as 100% relative sensitivity

speed, argon flow, T_i and T_p. The blank-corrected signals for each GLS demonstrate that the PE GLS is 2.75 times more efficient than the PSA1 GLS and is 3.20 times more efficient than the PSA2 GLS. The associated blank-corrected signals obtained and precision data are shown in Table 1.

Effect of Carrier Acidity

The PE GLS was used to examine the effect of varying carrier acidity from 0 (distilled, de-ionized water) to 10% v/v hydrochloric acid. While there was a steady decrease in the blank values obtained for decreased carrier acidity, the signal remained constant and then dropped slightly for a water carrier. This trend resulted in a maximum blank-subtracted sensitivity for a 1% hydrochloric acid carrier. This trend is shown in Fig. 7.

Table 1 Comparison of signals obtained with three different GLSs for optimized conditions of reagent and argon flow rates and injection and post-injection purge times. The injected sample was 500 μl of 20 ng ml^{-1} of Hg^{II} in 10% v/v hydrochloric acid. The carrier was 10% v/v hydrochloric acid and the reductant was 10% m/v tin(II) chloride in 10% v/v hydrochloric acid. All peak heights and integrated signals shown are blank-corrected

	Peak height		Integrated signal	
GLS	Mean	RSD (%)	Mean/s	RSD (%)
PE	0.3506	1.4 (n=5)	1.7406	1.2 (n=5)
PSA1	0.1275	1.8 (n=4)	0.6320	2.8 (n=4)
PSA2	0.1095	1.4 (n=4)	0.5436	2.1 (n=4)

Effect of Standard Solution Preservative Used

The results for the variation of blank signal as a function of carrier acidity indicated that the standard solution preservative employed might be a source of excess background Hg. A Hg standard solution preservative described by Welz *et al.*[17] involves adding 1 ml of a 50% nitric acid–0.5% $K_2Cr_2O_7$ solution to every 100 ml of aqueous Hg standard, giving a preservative concentration of 0.5% nitric acid and 0.005% $K_2Cr_2O_7$ at the point of analysis. This resulted in no decrease in signal values and a slight decrease in blank values compared with the signals and blanks obtained with the 10% hydrochloric acid preservative and 1% hydrochloric acid carrier.

Effect of Reductant Type Used

The 10% m/v tin(II) solution reductant employed for the optimization procedure was replaced with 1% m/v sodium tetrahydroborate solution to examine its effect on separation efficiency. It should be noted that a different manifold of identical design to that shown in Fig. 1 was used. This was necessary since the introduction of sodium tetrahydroborate into a manifold used for tin(II) reductions will result in the precipitation of elemental tin. Using the optimized parameters found with tin(II), there was no difference in peak height sensitivity relative to the tin(II) reductant when the sodium tetrahydroborate reductant was used with the PE GLS. However, there was a 36% decrease in integrated signal sensitivity for the sodium tetrahydroborate reductant compared with that obtained with the tin(II) reductant for the PE GLS. A major difference between the use of tetrahydroborate and the use of tin is that the acid decomposition of the excess tetrahydroborate generates copious amounts of hydrogen. It is possible that the constant formation of hydrogen, even with the argon purge deactivated, leads to greater overall pressure in the system. This would result in decreased residence time of the Hg vapour in the atom cell and a decrease in integrated signal for the sodium tetrahydroborate reductant, without necessarily leading to a decrease in peak height. Thus it it difficult to make direct comparisons between these two reductants due to the presence of the hydrogen.

While the peak height sensitivity might have been unchanged, it has been noted[26] that using sodium tetrahydroborate in determinations of Hg with amalgam concentration can lead to poisoning of the trapping medium from adsorption of metal hydrides generated from background elements (*i.e.*, arsenic and selenium) in the sample. This results in fewer surface active sites for the liberated Hg vapour to form an amalgamation, thus leading to lower trapping efficiency and lower sensitivity. It has also been noted[27] that the presence of transition metals [specifically copper(II)] can lead to depression of the Hg signal when using sodium tetrahydroborate as a reductant. It was

Table 2 Optimized conditions for Hg vapour generation using the PE GLS by flow injection analysis. All flow rates shown are in ml min^{-1}. The sample was 500 μl of 20 ng ml^{-1} of Hg^{II}. The optimized injection time (T_i) was 25 s and the optimized post-injection purge time (T_p) was 10 s

Reagent	Concentration	Flow rate
Ar purge	—	250
Carrier	1% v/v HCl	3.5
Reductant	10% m/v $SnCl_2$ in 10% v/v HCl	1.5
Standard preservative	0.005% m/v $K_2Cr_2O_7$ in 0.5% v/v HNO_3	—

deduced that the elemental Hg adsorbs on the surface of the finely divided copper precipitate that is also formed in the reduction process. For optimum sensitivity and the relative freedom from interference effects compared with sodium tetrahydroborate, tin(II) was determined to be the better reductant. Optimized parameters are shown in Table 2.

Comparison of the PE GLS Using a Calculated Mass of Hg With Amalgam Preconcentration

The apparatus shown in Fig. 3 was used to introduce a calculated mass of Hg vapour into the gold–platinum gauze prior to thermal desorption and detection. By making injections of the Hg-saturated air onto the gold gauze, along with the analysis of argon blank values, the system is calibrated in terms of the mass of Hg introduced. The mass of Hg introduced is calculated by using the data for Hg vapour pressures reported by Weast *et al.*[28] At a temperature of 24 °C, 500 μl of saturated air contains 9.2 ng of Hg vapour. A 500 μl sample of 20 ng ml^{-1} of Hg^{II} (10.0 ng) was then injected into the optimized FI-CVAAS system with an amalgam concentration unit, with the signals and the blanks being measured. The results obtained from the system containing the amalgam trap, calibrated by the introduction of Hg vapour of calculated mass, demonstrated that the PE GLS was $103 \pm 6\%$ (95% confidence interval) efficient by integrated signal measurements and $101 \pm 4\%$ (95% confidence interval) efficient by peak height measurements.

Conclusions

It has been shown under optimized conditions that the efficiency of Hg vapour separation in FI-CVAAS is variable and is dependent upon the design of the gas–liquid separator. The most efficient gas–liquid separator examined in this study was shown to achieve complete separation based upon a Hg vapour mass calibration of an amalgam concentration accessory. As it is known that the measures taken in the optimization process to ensure maximum separation efficiency (*e.g.*, lower reagent flow rates, higher argon purge flow rates) would lead to a decrease in sensitivity if amalgam preconcentration was not used, the sensitivity of an FI-CVAAS manifold using amalgam preconcentration reaches a maximum value, which is based upon the efficiency of the vapour separation process. It is thus apparent that the amalgam preconcentration process successfully decouples the kinetics of the FI-CVAAS manifold from the atomic spectrometer. This study also shows that a decrease in internal volume of the gas–liquid separator does not necessarily lead to incomplete gas–liquid separation, as some workers have stated.[29]

Financial support for this work and the provision of equipment by The Perkin-Elmer Corporation is gratefully acknowledged.

References

1 El-Awady, A. A., Miller, R. B., and Carter, M. J., *Anal. Chem.*, 1976, **48**, 110.
2 Agemian, H., and Chau, A. S. Y., *Anal. Chem.*, 1978, **50**, 13.
3 Jirka, A. M., and Carter, M. J., *Anal. Chem.*, 1978, **50**, 91.
4 Oda, C. E., and Ingle, J. E., Jr., *Anal. Chem.*, 1981, **53**, 2030.
5 Goto, M., Shibakawa, T., Arita, T., and Ishii, D., *Anal. Chim. Acta*, 1982, **140**, 179.
6 de Andrade, J. C., Pasquini, C., Baccan, N., and Van Loon, J. C., *Spectrochim. Acta, Part B*, 1983, **38**, 1329.
7 Morita, H., Kimoto, T., and Shimomura, S., *Anal. Lett.*, 1983, **16**, 1187.
8 Anderson, P. J., *At. Spectrosc.*, 1984, **5**, 101.
9 Fang, Z., Xu, S., Wang, X., and Zhang, S., *Anal. Chim. Acta*, 1986, **179**, 325.
10 Fang, Z., Zhu, Z., Zhang, S., Xu, S., Guo, L., and Sun, L., *Anal. Chim. Acta*, 1988, **214**, 41.
11 Goto, M., Munaf, E., and Ishii, D., *Fresenius' Z. Anal. Chem.*, 1988, **332**, 745.
12 Birnie, S. E., *J. Automatic Chem.*, 1988, **10**, 140.
13 Pasquini, C., Jardim, W. F., and de Faria, L. C., *J. Automatic Chem.*, 1988, **10**, 188.
14 Nakahara, T., Kawakami, K., and Wasa, T., *Chem. Express*, 1988, **3**, 651.
15 Nakahara, T., and Wasa, T., *Microchem. J.*, 1990, **41**, 148.
16 Munaf, E., Takeuchi, T., and Haraguchi, H., *Fresenius' Z. Anal. Chem.*, 1992, **342**, 154.
17 Welz, B., Tsalev, D. L., and Sperling, M., *Anal. Chim. Acta*, 1992, **261**, 91.
18 Baxter, D. C., and Frech, W., *Anal. Chim. Acta*, 1990, **236**, 377.
19 Barnes, R. M., and Wang, X., *J. Anal. At. Spectrom.*, 1988, **3**, 1083.
20 Wang, X., and Barnes, R. M., *J. Anal. At. Spectrom.*, 1988, **3**, 1091.
21 Welz, B., Melcher, M., Sinemum, H. W., and Maier, D., *At. Spectrosc.*, 1984, **5**, 37.
22 Thompson, M., Pahlavanpour, B., Walton, S. J., and Kirkbright, G. F., *Analyst*, 1978, **103**, 568.
23 Kaseke, C. T., M.Sc. Thesis, Loughborough University of Technology, UK, 1977.
24 Dumarey, R., Temmerman, E., Dams, R., and Hoste, J., *Anal. Chim. Acta*, 1985, **170**, 337.
25 Temmerman, E., Vandecasteele, C., Vermeir, G., Leyman, R., and Dams, R., *Anal. Chim. Acta*, 1990, **236**, 371.
26 Welz, B., and Schubert-Jacobs, M., *Fresenius' Z. Anal. Chem.*, 1988, **331**, 324.
27 McIntosh, S., unpublished data.
28 *CRC Handbook of Chemistry and Physics*, ed. Weast, R. C., CRC Press, Cleveland, 52nd edn., 1971.
29 Fang, Z., in *Flow Injection Atomic Spectroscopy*, ed. Burguera, J. L., Marcel Dekker, New York, 1989, ch. 4.

Paper 2/06779J
Received December 12, 1992
Accepted January 22, 1993